Associations between large-scale atmospheric circulation and polar lows developments over the North Atlantic during winter

Chantal Claud, Bertrand Duchiron, Pascal Terray

Associations between large-scale atmospheric circulation and polar low developments over the North Atlantic during winter

Chantal Claud,[1] Bertrand Duchiron,[1] and Pascal Terray[2]

Received 14 November 2006; revised 20 March 2007; accepted 6 April 2007; published 16 June 2007.

[1] Polar lows are intense mesoscale weather systems which develop in response to combinations of upper tropospheric vorticity advection, low-level baroclinicity near the sea ice-ocean margin and strong air-sea thermodynamical fluxes. In this paper, an evaluation of the associations between dominant patterns of low-frequency variability in the atmospheric circulation and polar low developments over the North Atlantic during winter is presented. Because polar lows are rather poorly represented in reanalyses, the temperature (T500) and geopotential height at 500 hPa, the wind at 925 hPa, the SST, and the difference (SST-T500), which are critical for their formation, are considered. The North Atlantic Oscillation (NAO) has a strong impact on all these variables, but it is contrasted spatially and temporally. Polar low formation is stimulated in the Labrador Sea for a positive NAO phase, while over the Norwegian Sea, there is an increase of polar lows forming on the flank of synoptic storms. Still over the Norwegian Sea, higher SST from January on favor the formation of polar lows of predominantly convective nature, while to the east of Greenland, the reduction of sea ice plus the northerly low-level flow lead to a larger number of polar lows. Other teleconnection patterns also exhibit associations with polar low developments. The Scandinavia pattern shows a strong negative association with the studied variables over the Norwegian and Barents seas, but only marginally affects the Labrador Sea. The formation of polar lows is encouraged over the Norwegian and Greenland seas when the Polar/Eurasia pattern is in its negative phase.

Citation: Claud, C., B. Duchiron, and P. Terray (2007), Associations between large-scale atmospheric circulation and polar low developments over the North Atlantic during winter, *J. Geophys. Res.*, *112*, D12101, doi:10.1029/2006JD008251.

1. Introduction

[2] The North Atlantic region is prone to the development of intense mesoscale maritime weather systems called polar lows which form during wintertime when very cold air is transported over relatively warm open sea. It has been known for a long time that the Norwegian and Barents Seas are preferred regions for their development [e.g., *Rasmussen and Turner*, 2003]; however the occurrence of polar lows is not limited to these particular areas and such cyclones may form in several places around the world, provided that very cold air is advected out over relatively warm water. A rather southern genesis region is found over the Labrador Sea between the east coast of Labrador and southwestern Greenland [*Rasmussen et al.*, 1996]. The eastern Canadian waters (Davis Strait, Baffin Bay and Hudson Bay) are also genesis regions and occasionally, during intense cold northerly outbreaks, the north of the United Kingdom is prone to polar lows too [*Hewson et al.*, 2000]. Considerable insight into the structure and dynamics of polar lows has followed advances in remote sensing techniques [e.g., *Claud et al.*, 1993, 2004; *Carleton et al.*, 1995; *Heinemann*, 1996; *Rasmussen et al.*, 1996; *McMurdie et al.*, 1997; *Lieder and Heinemann*, 1999]. There is a range of conditions leading to the development of such systems, sometimes referred to as the "polar low spectrum" [*Rasmussen and Turner*, 2003]. However, observational and model studies have both shown that a predevelopment condition is provided by an outbreak of very cold air flowing from an ice or land surface over a warmer water surface, therefore providing strong surface heat fluxes and reduced low-level stability. In addition, a number of polar lows are triggered by the approach of an upper level system under the form of a potential vorticity (PV) anomaly or a cold upper trough, which initiates deep convection by decreasing stability [*Rasmussen and Turner*, 2003, and references therein].

[3] The relatively small scale of these systems (typical size in the range 100–1000 km) added to their relatively short life time (one to two days) present some concern as to their representation in the meteorological reanalysis data sets. Recently, *Condron et al.* [2006] have shown that a large portion of these systems is not represented in ERA-40 data (about 3 out of 4 for polar lows having a size between 100 and 500 km). It probably explains to a certain extent why so far the relationship of polar lows to large-scale atmospheric circulation has not been investigated in detail. Nevertheless, with surface winds which can be in excess of

[1] Laboratoire de la Meteorologie Dynamique/Institut Pierre-Simon Laplace, Ecole Polytechnique, Palaiseau, France.
[2] Laboratoire d'Océanographie et du Climat: Expérimentations et Approches Numériques/Institut Pierre-Simon Laplace, Paris, France.

0148-0227/07/2006JD008251

30 m/s, they are associated with large turbulent fluxes. Given that they tend to cluster temporally and spatially, polar lows may assist deep water formation in regions such as the East Greenland and Labrador Seas [e.g., *Hakkinen*, 1995]. They are therefore an important component of the coupled atmosphere-ocean system. Documenting the synoptic-climatological environments favorable to the development of polar lows is thus relevant not only for medium- to long-range forecasting but also for understanding climate variability. This is even more true in the context of climatic change in which the impact of global warming in the Arctic on severe weather over this area remains to be assessed.

[4] A variety of teleconnection patterns which refer to persistent and recurring large-scale pressure and circulations over the globe have been defined using monthly mean 700 hPa heights [*Barnston and Livezey*, 1987]. These patterns represent preferred modes of atmospheric variability that last for a few weeks or months, and influence temperature, precipitation, storm tracks, location and intensity of the jet stream. Several teleconnection patterns have been observed over the northern Atlantic during the cold season, and may therefore be associated with polar low formation. A primary teleconnection pattern is the North Atlantic Oscillation (NAO), which is represented by changes in the intensity of the westerly circulation in middle and higher latitudes of the North Atlantic/Europe sector. In the NAO positive phase, below normal pressure over Greenland and the high latitudes of the North Atlantic, and higher than normal pressure over western Europe is observed. This explains why for high-latitude regions, these have sometimes been called the GA (Greenland Above temperature) and GB (Greenland Below temperature) patterns [*van Loon and Rogers*, 1978; *Rogers and van Loon*, 1979], which correspond to negative and positive phases of the NAO, respectively. In addition to the NAO, there are other regional teleconnection patterns. The positive index of the Scandinavia (SCAND) pattern is associated with a blocking high over Scandinavia, which pushes the storm track south over Europe, while the negative phase corresponds to anomalously low pressure in Scandinavia and high pressure over western Europe. The Polar/Eurasia (POLASIA) pattern is a dominant mode of low-frequency atmospheric variability in winter, which reflects changes in the strength of the circumpolar circulation. The positive phase is dominated by lower than normal pressure over the polar region, an enhanced circumpolar vortex, and higher than normal pressure over Europe. The East Atlantic/West Russia (EAWR) pattern brings lower than normal pressure and colder drier air over the eastern North Atlantic and Europe during its negative phase, which will lead to an intensification of the storm track or local cyclogenesis over the southeastern part of the area. Finally, the East Atlantic (EASTATL) pattern has some resemblance to the NAO but is centered further south. In its positive phase, synoptic activity is enhanced across the whole of the North Atlantic, but does not penetrate into the Nordic Seas (i.e., the northeast Atlantic east of Greenland and north of 60°N, the Greenland Sea, the Norwegian Sea, the Barents Sea and the North Sea).

[5] The association of polar lows with changes in the locations and amplitude of planetary waves [e.g., *Forbes and Lottes*, 1985], SST anomalies, sea-air temperature difference and sea ice extent provides a context for a low-frequency signature associated with major climatic teleconnection patterns. Rather surprisingly, these low-frequency associations of polar lows have been better studied for the Southern Hemisphere than for the Northern Hemisphere [*Carleton*, 1996]. Moreover the few studies for the Northern Hemisphere are restricted to short periods of time (typically a couple of years characterized by contrasting climate and circulation conditions). *Carleton* [1985, 1996] analyzed satellite imagery in conjunction with surface and upper air synoptic observations for two years (December-January-February) in order to derive climatological information on polar lows. He observed during GB winter (positive NAO phase) that (1) more systems develop east of Labrador and Newfoundland, (2) the mesoscale cyclones that form in the Norwegian Sea have a strong northward component to system motion, and (3) a larger number of mesocyclones form near Greenland. *Harold et al.* [1999], using a 2-year database compiled from infrared satellite imagery, studied polar mesocyclone activity over the Northeast Atlantic (polar mesocyclones are sub-synoptic-scale low pressure systems which form over high-latitude oceans, the most vigorous being polar lows). These authors found that the number of cyclones with a size in the range 200–600 km increases as the NAO index becomes more positive, and related this result to a response of the formation of polar mesocyclones to enhanced synoptic cyclone activity in the central Nordic Seas area. Their study also indicated that in winter, formation of midsized mesocyclones (200 to 600 km wide) is encouraged when the polar vortex is weak, suggesting cyclogenesis in off-ice flow from the Arctic and Barents Sea ice sheets caused by anticyclonic conditions over the Arctic and Greenland. Recently, *Kolstad* [2006], also related the NAO to reverse shear polar lows [*Duncan*, 1977], which represent a specific type of polar lows, in which the low-level winds are antiparallel to the thermal wind in adjoining layers.

[6] The objective of this study is to extend the previous studies by examining statistically over a sufficiently long period of time the relationships between teleconnection patterns and polar low activity. The existence of the so-called reanalyses, which consist of long global data records, should enable one to reconsider this question, but, as mentioned above, because of the relatively poor representation of polar lows, it is rather the association between these patterns and surface and atmospheric variables important for polar lows developments that will be assessed. A number of studies concerning the occurrence of polar lows and the large-scale environment in which they tend to form have been carried out over the years in and around the Nordic Seas [e.g., *Businger*, 1985, 1987; *Ese et al.*, 1988; *Parker*, 1991, 1997; *Rasmussen et al.*, 1996]. Several variables have thus been identified as key factors for the development and therefore the forecasting of polar lows [*Noer and Ovhed*, 2003]. Since many polar lows are triggered by cold, upper level troughs, the temperature and the geopotential height at 500 hPa are considered (a value of −39°C is generally considered as a threshold). Cold air outbreak occurrence is investigated through the study of wind at 925 hPa. The SST is a critical variable for at least two reasons: first, several polar lows form at the sea

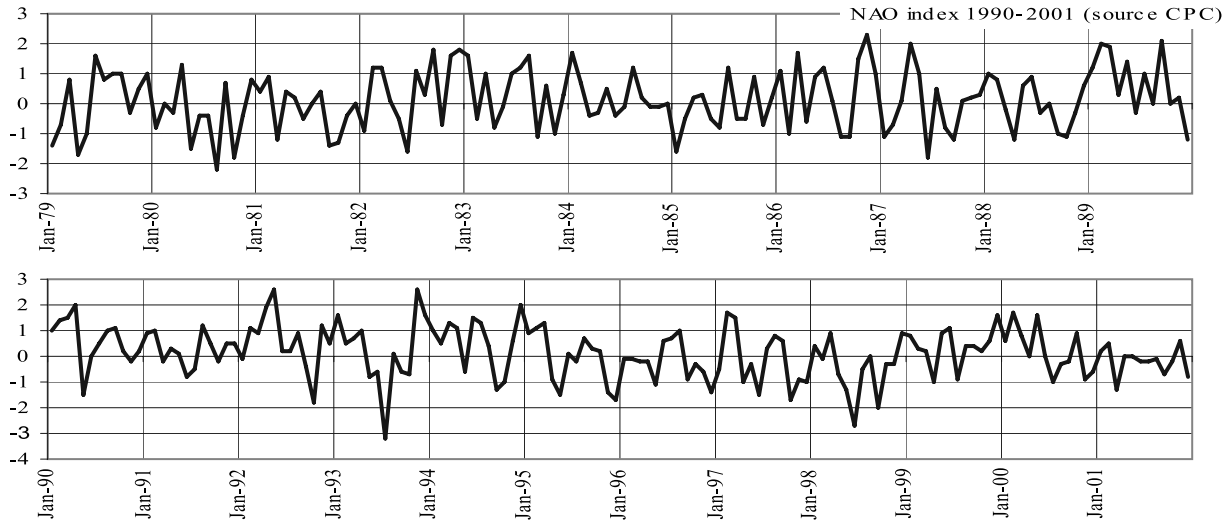

Figure 1. Temporal evolution of the NAO monthly index between January 1979 and December 2001.

ice margin, in connection with preexisting shallow boundary layer fronts; second, because of the importance of thermodynamical fluxes for their intensification. A number of numerical studies have shown that without the contribution of the latter, polar lows would not develop beyond the stage of a moderately strong trough [e.g., *Emanuel and Rotunno*, 1989; *Claud et al.*, 2004]. In addition, the difference between the SST and the temperature at 500 hPa is used as an indicator of the static stability, such that strongly positive values indicate instability and convection from the surface (45°C is often taken as a threshold value [*Noer and Ovhed*, 2003]). Finally, the wind at 300 hPa is also considered because several polar lows may form within the parent circulation of a synoptic-scale occluded cyclone [*Rasmussen and Turner*, 2003].

[7] A statistical analysis of these variables, as provided by ERA-40 [*Simmons and Gibson*, 2000] and NCEP R-2 [*Kanamitsu et al.*, 2002] reanalyses, is carried out. We employ the monthly mean data covering the period 1979–2001. Although data exist over a longer period for the previous NCEP-NCAR reanalysis [*Kalnay et al.*, 1996] and for ERA-40, we choose to use only the period after 1979, since use is made of satellite data (possible shifts due to their use are therefore avoided). Geographically, this study concentrates on the North Atlantic Sector.

[8] The paper is organized as follows. In section 2, the data and the method are presented. In section 3, associations between large-scale circulation as reflected by the different teleconnection indices and tropospheric fields important to polar low developments are presented. Finally, the results from the analysis are summarized and discussed in section 4.

2. Data and Method

2.1. ERA-40 Reanalysis

[9] The ERA-40 data assimilation system [*Simmons and Gibson*, 2000] uses the Integrated Forecasting System (IFS) developed jointly by ECMWF and Météo-France. A three-dimensional variational method is used to assimilate the observations into the spectral model, which has 60 vertical levels and T159 horizontal spectral resolution. Since 1979, the reanalysis makes comprehensive use of satellite observations. Data are available for 23 pressure levels with a spatial resolution of 1.125°. A more detailed description of the ERA-40 data set can be obtained online at http://www.ecmwf.int/research/era.

2.2. NCEP/NCAR Reanalysis

[10] Use was also made of the NCEP R-2 reanalysis data [*Kanamitsu et al.*, 2002] to characterize the links between the large-scale circulation and polar lows. The reanalysis is available from January 1979 through December 2001. The model is run at a horizontal resolution of T62, with 28 vertical levels. Geopotential heights, temperatures and winds in the troposphere are available at 12 pressure levels from 1000 to 100 hPa. Data are given on a $2.5 \times 2.5°$ latitude/longitude grid.

2.3. Sea Surface Temperatures

[11] Despite of the fact that SST are available in these two reanalyses, we have also considered Extended reconstructed SST (ERSST), which correspond to a monthly extended reconstruction of global SST based on Comprehensive Ocean-Atmosphere Data Set and underwent a rigorous quality control [*Smith and Reynolds*, 2003, 2004]. In addition, sea ice concentrations have been used to improve high-latitude SST analysis. SST are available on a 2° spatial grid at: http://lwf.ncdc.noaa.gov/oa/climate/research/sst/sst.html#ersst.

2.4. Teleconnection Patterns Indices

[12] The indices were taken from http://www.cpc.ncep.noaa.gov/data/teledoc/telecontents.shtml. As an example, the temporal evolution of the NAO index can be seen in Figure 1. Because this index is not necessarily persistent over the whole cold season (Figure 1), we have chosen to consider a monthly index rather than an annual index; this holds also for the other indices.

2.5. Method

[13] To characterize the associations between low-frequency patterns and polar low developments, standard

Table 1. Correlation Coefficients Between the Different Indices for Months Between November and March[a]

	POLASIA	*NAO*	*SCAND*	*EASTATL*	*EAWR*
			November		
POLASIA	1.000				
NAO	−0.063	1.000			
SCAND	0.244	0.146	1.000		
EASTATL	−0.134	0.097	0.168	1.000	
EAWR	0.092	−0.029	−0.038	−0.203	1.000
			December		
POLASIA	1.000				
NAO	0.072	1.000			
SCAND	0.289	0.054	1.000		
EASTATL	−0.004	−0.074	0.047	1.000	
EAWR	**0.386**	0.048	0.183	0.046	1.000
			January		
POLASIA	1.000				
NAO	−0.251	1.000			
SCAND	−0.085	**−0.360**	1.000		
EASTAL	−0.256	0.333	0.147	1.000	
EAWR	0.245	−0.165	−0.275	0.009	1.000
			February		
POLASIA	1.000				
NAO	−0.334	1.000			
SCAND	0.207	−0.299	1.000		
EASTATL	−0.204	0.179	−0.265	1.000	
EAWR	0.001	−0.058	−0.076	0.230	1.000
			March		
POLASIA	1.000				
NAO	0.034	1.000			
SCAND	0.258	−0.342	1.000		
EASTATL	0.108	−0.210	**−0.443**	1.000	
EAWR	−0.122	0.152	0.019	−0.182	1.000

[a]Values in bold are significant at the 90% level.

cross-correlation and regression techniques between the corresponding indices and atmospheric fields have been performed. The statistical significance of the results has been assessed with a phase-scrambling bootstrap test with 999 samples [*Davison and Hinkley*, 1997], taking into account the autocorrelation characteristics of the time series. The associations will be shown separately for months from November through March, which corresponds to the period of polar lows maximum occurrence. Key variables for the development of polar lows include the 500 hPa temperature (T500) and geopotential height (for the determination of enhanced potential vorticity), the low-level wind (indicative of cold air outbreaks), the Sea Surface Temperature (SST), and the difference between the SST and the temperature at 500 hPa (SST-T500). The wind at 300 hPa was also investigated because polar lows can form as a result of convective instability in cold air flowing over a warm ocean during a cold air outbreak, after the passage of a synoptic depression.

[14] Although the results are shown for the whole area poleward of 45°N, results are discussed only for a domain situated north of 60°N, and from 60°W to 60°E. In particular, associations with polar lows over the North Pacific Basin are not discussed here, since they should include other teleconnection patterns like the El Nino Southern Oscillation [*Yarnal and Henderson*, 1989a, 1989b]. Besides, since polar lows are maritime weather systems, results are discussed only over open sea.

[15] Correlation coefficients between the different indices for the period 1979–2001 have been determined for months between November and March (Table 1). Significant correlations have been obtained for POLASIA and EAWR in December (0.386), NAO and SCAND in January (−0.360), and SCAND and EASTATL in March (−0.443). For this reason, as an example, in December, partial correlation analysis is first performed with EAWR and the anomalies associated with EAWR substracted from the full signal prior to the correlation with POLASIA (and vice versa). A similar procedure is used for the other cases of significant correlation.

3. Associations Between Teleconnection Patterns and Surface and Atmospheric Fields Over the North Atlantic

3.1. NAO

3.1.1. The 500 hPa Temperature and Height

[16] Figure 2 presents the correlations between the NAO index and the temperature at 500 hPa derived from ERA-40. For the five winter months, a positive phase of the NAO corresponds to a significant cooling of a large area centered approximately over the Davis Strait and south Greenland and including the Labrador Sea and Newfoundland, favorable for polar low developments in these subregions [*Carleton*, 1988]. Correlations reach −0.7; −0.8; conversely, it corresponds to warmer temperatures over the eastern part of our domain (correlations of about 0.5; 0.6) resulting in less favorable conditions for the development of polar lows. There are however regional differences depending on the month: in November and December, there is no significant positive correlation in the polar low genesis regions. In January and March, significant positive correlations are found over the Barents and Kara Seas, while in February they cover a portion of the Norwegian Sea. Correlations between the NAO index and ERA-40 500 hPa geopotential heights (not shown) have also been determined. Large-scale patterns of 500 hPa geopotential heights are in line with temperature patterns. The negative 500 hPa temperature and height patterns indicate a positive potential vorticity anomaly and the potential for deep convection over the area.

[17] Correlations between the NAO index and the 500 hPa temperature deduced from NCEP-R2 are presented in Figure 3, and illustrate the high degree of similarity between the results obtained by the two reanalyses. Patterns agree to a large extent; it is only the significant areas which differ slightly; in the following, we will therefore just show and discuss correlations with ERA-40 fields, which have better vertical and spatial resolutions.

3.1.2. The 925 hPa Wind

[18] Figure 4 displays regression patterns of the NAO index and the corresponding ERA-40 reanalyzed 925 hPa wind for winter months. Only features that exhibit correlations exceeding the 90% confidence level are displayed. For the whole winter, a positive NAO phase is associated with northerly to westerly winds over the Labrador Sea and the eastern Canadian waters (more significant in November-January-March). East of Greenland, from December onward, the positive phase corresponds also to northerly or

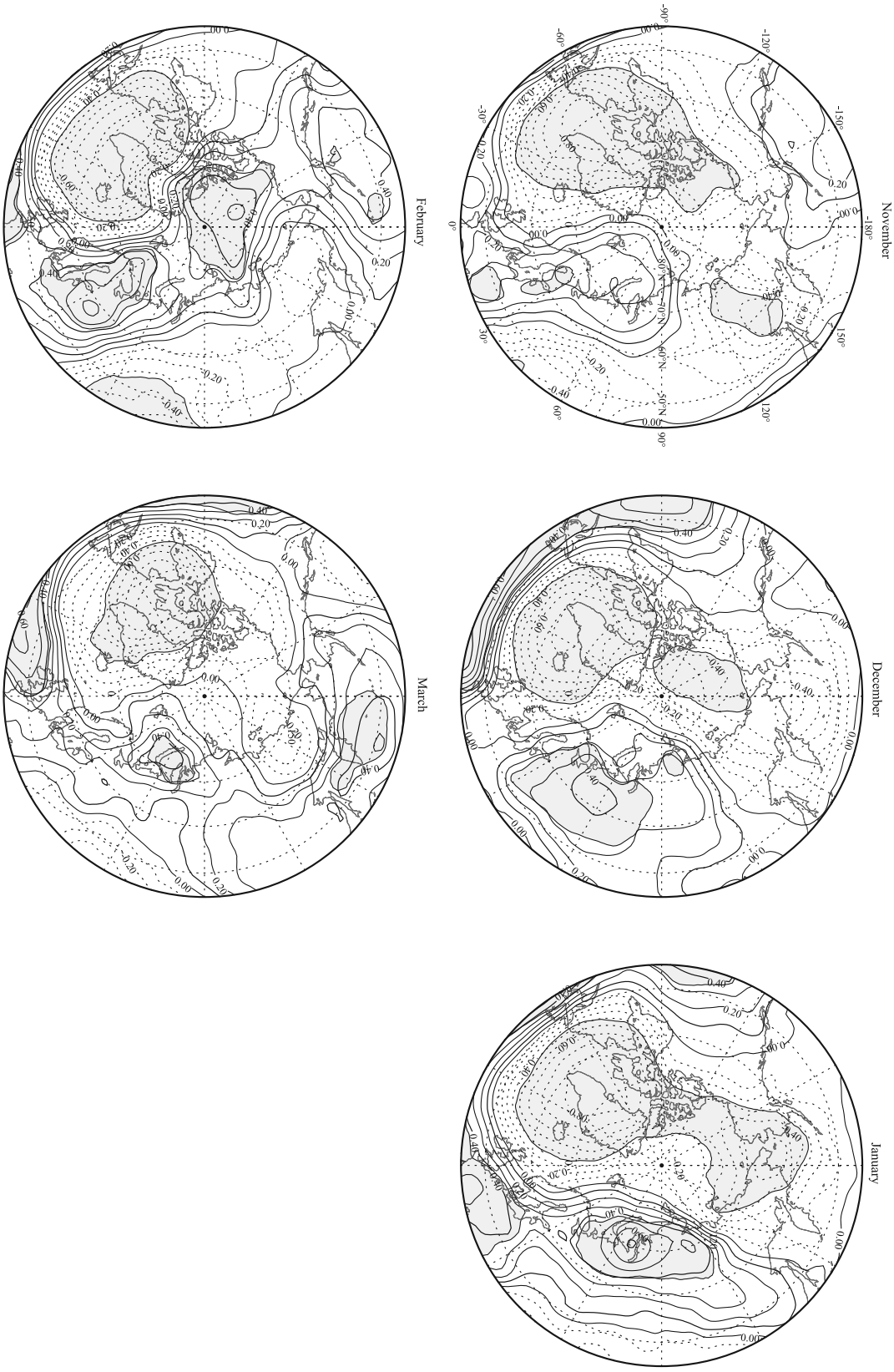

Figure 2. Distribution of correlation coefficients of ERA-40 500 hPa temperature between November and March versus the NAO index. Correlation coefficients have been computed for the 1979–2001 period. Correlation coefficients above the 90% confidence level following a phase-scrambling procedure with 999 samples are shaded. See text for more details.

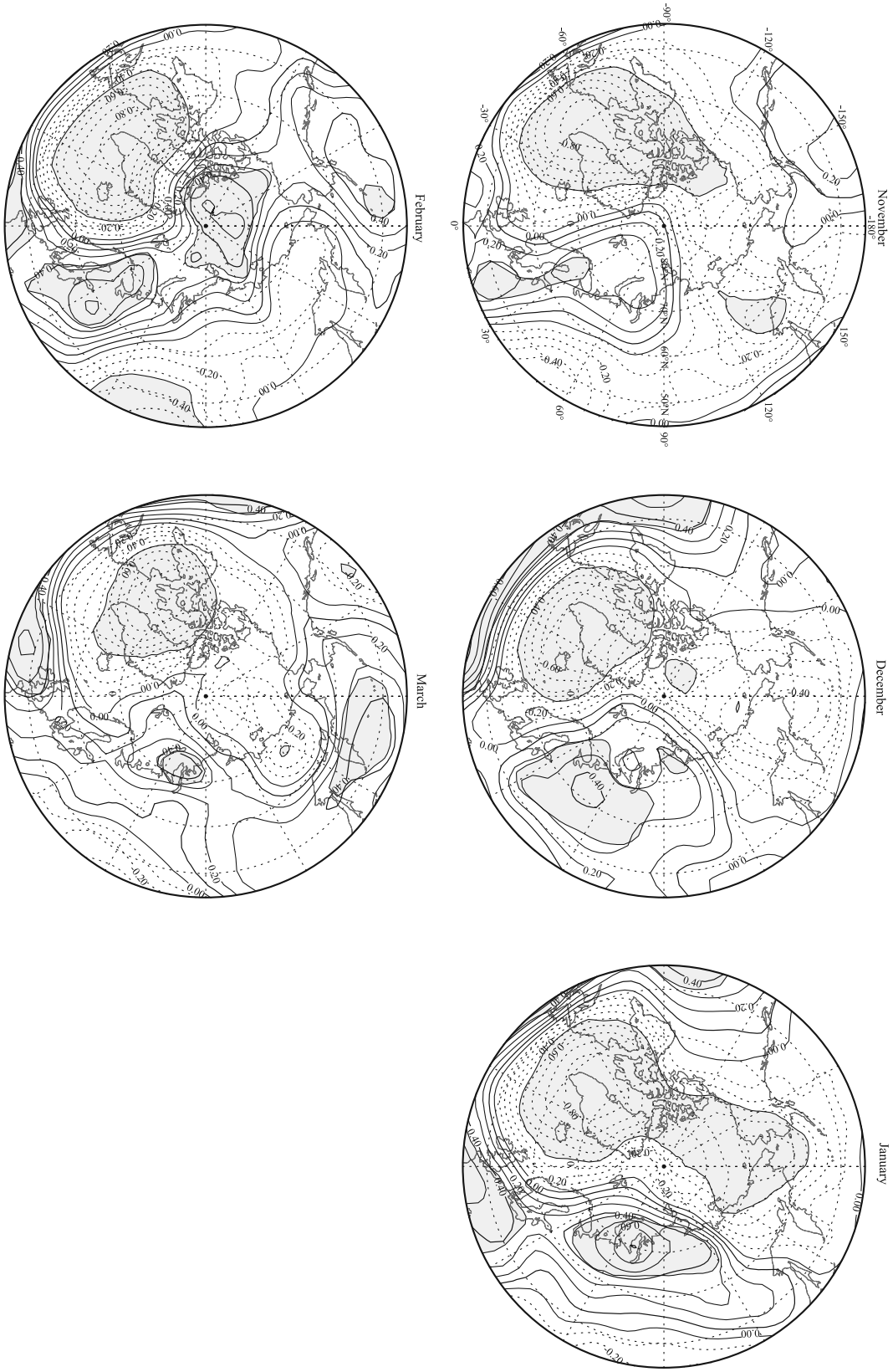

Figure 3. Same as Figure 2 but for NCEP R-2 reanalysis.

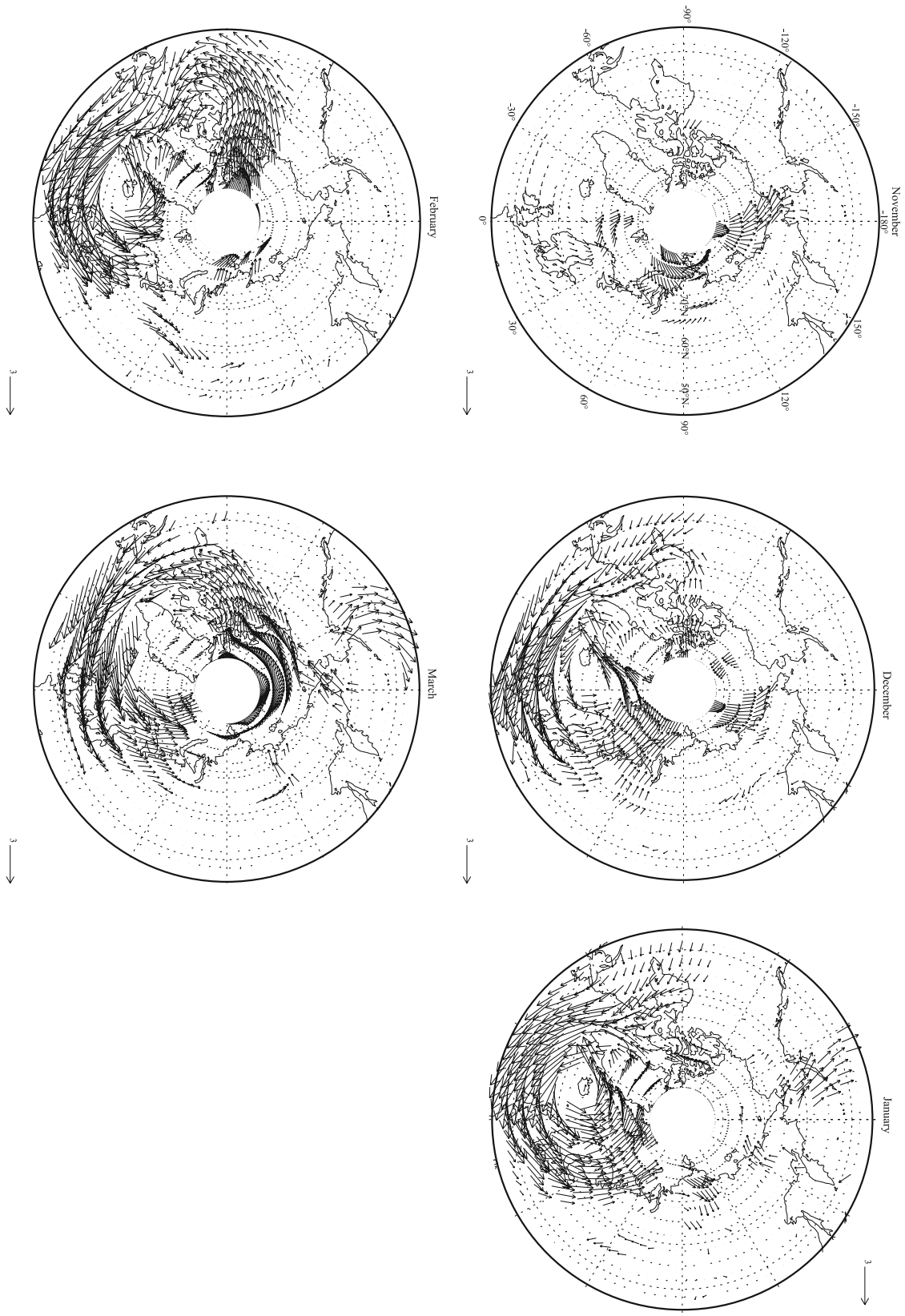

Figure 4. Distribution of monthly regression coefficients of ERA-40 925 hPa wind between November and March versus the NAO index. Regression coefficients have been computed for the 1979–2001 period, and only 1 out of 3 wind vectors are plotted. Maps only show wind vectors corresponding to regression coefficients above the 90% confidence level following a phase-scrambling procedure with 999 samples. See text for more details.

northeasterly winds. These positive correlations reflect favorable conditions for polar low developments. A positive NAO phase is conducive to southerly or southwesterly winds over most of the Norwegian and Barents Seas. These will favor the development of synoptic storms coming from the southwest that are likely to be followed by reverse shear conditions, as shown by *Kolstad* [2006].

3.1.3. SST

[19] In agreement with previously published studies, a strong association between the NAO and SST is observed during winter months, as can be seen on Figure 5. Consistently over the 5 months, there is a reduction of sea ice to the east of Greenland [e.g., *Rigor et al.*, 2002]. An indirect effect of this sea ice reduction is that the boundary layer is less stably stratified over the Nordic and Barents Sea [*Wu et al.*, 2004]. There is also a negative correlation area over the North Atlantic that is significant for all months, except February. In addition, from January onward, there is a positive correlation all along the Norwegian coast with correlation coefficients larger than 0.4, especially in February. Conversely, over the Labrador Sea, negative correlations are observed (significant in December and January and higher than 0.6 for this latter month).

3.1.4. SST-T500

[20] Figure 6 displays the correlations between the NAO index and the variable (SST-T500) for winter months. Positive correlations are observed over the Barents and Kara Seas during the whole period, over the Norwegian and Greenland Sea in December-January-February, and over the Labrador Sea in January. However, the correlations are hardly significant, except in December north of 65°N. Conversely, negative correlations are observed over the Denmark Strait in December and over the Labrador Sea for the whole season except January.

3.1.5. The 300 hPa Wind

[21] Because several polar lows form within the parent circulation of a synoptic-scale occluded low, the wind at 300 hPa has also been considered. A positive phase of the NAO is associated with west-southwesterly 300 hPa winds over the north Atlantic (not shown), leading to an increased likelihood of synoptic-scale storms, and therefore of polar lows over the Norwegian Sea.

3.2. Other Teleconnection Patterns

[22] In the following, the emphasis will be put on the major significant patterns. In addition, as observed for the NAO, there is a high degree of similarity between the 500 hPa temperature and geopotential height results. For this reason, geopotential height results are not shown or discussed, but a negative (positive) correlation with T500 also means a negative (positive) correlation with the 500 hPa geopotential height.

3.2.1. Scandinavia Pattern

[23] The positive phase of the Scandinavia pattern corresponds to the presence of a blocking high over Scandinavia. This teleconnection pattern exhibits a strong significant correlation with T500 (coefficients of about 0.7) with higher temperatures over most of the Norwegian and Barents Seas in the case of a positive index (Figure 7a, valid for December). In February (Figure 7b) and March, the warmer area is centered over the Norwegian Sea, while it is situated further northeast for the other months.

[24] This pattern also shows a strong association with 925 hPa wind over the northeast Atlantic. A positive phase is associated with southeasterly winds over the Norwegian Sea in November-December (Figure 7c), and southerly winds over the Greenland Sea from January onward. This corresponds to a decreased likelihood of polar lows over this area. Conversely, the Kara Sea, and the Barents Sea are characterized by northerly winds from January onward (Figures 7d–7e).

[25] Among all other teleconnection patterns, the Scandinavian pattern shows the strongest association with SST. In February (Figure 7f) and March, a positive index corresponds to decreased SST along the western coast of northern Europe, that is opposite to the NAO results, with correlations as high as 0.6 in February. At the beginning of the winter season, the Norwegian Sea and part of the Barents Sea exhibit a significant positive correlation.

[26] Concerning (SST-T500), the Scandinavia pattern exhibits mostly negative correlations (neutral in February), practically never significant except in November and March over the Barents Sea (not shown).

[27] For completeness, the Scandinavia pattern is associated with easterly 300 hPa winds over the north Atlantic during the period January–March (not shown), leading to a decreased likelihood of polar lows forming to the rear of synoptic-scale storms over the Norwegian Sea.

3.2.2. Polar/Eurasia Pattern

[28] A positive Polar Eurasian index, i.e., an enhanced circumpolar vortex, is generally associated with lower temperatures over the northernmost latitudes surrounded by higher values to the south. However, in December (Figure 8a) and March, large positive correlations of T500 with the Polar Eurasian index are obtained over the Norwegian Sea with values of 0.6 and higher and 0.4, respectively. There is no effect of the Polar/Eurasia pattern on polar low developments in eastern Canadian waters.

[29] A positive Polar Eurasian index is also associated with northerly or northwesterly winds over the Barents Sea during the whole winter (not shown). This is true for Baffin Bay and Davis Strait in December and March too. The correlation of the Polar Eurasian index with 925 hPa winds is low over the Greenland/Norwegian Sea, except in December, for which a positive index corresponds to southwesterly winds, which may generate reverse shear polar lows (see above), and in March with southerly winds which inhibit polar low activity.

[30] In January (Figure 8b) and February, the Polar Eurasian index and the SST are significantly correlated. Negative significant correlation areas are found over a broad area, west of Europe and covering part of the Barents Sea (values of −0.4 in January, smaller in February).

[31] Negative correlations between the Polar Eurasian index and (SST-T500) are observed over the Norwegian and Barents Sea; they are significant in November over the Barents Sea, in January (Figure 8c) over the Norwegian Sea and in February over the Greenland Sea. However, by the end of the polar low season, significant positive correlations are found over an area covering the Labrador Sea and to the west of the British Isles (Figure 8d).

3.2.3. East Atlantic/West Russia Pattern

[32] The positive phase of the East Atlantic/West Russia pattern is associated with warmer air over the eastern North

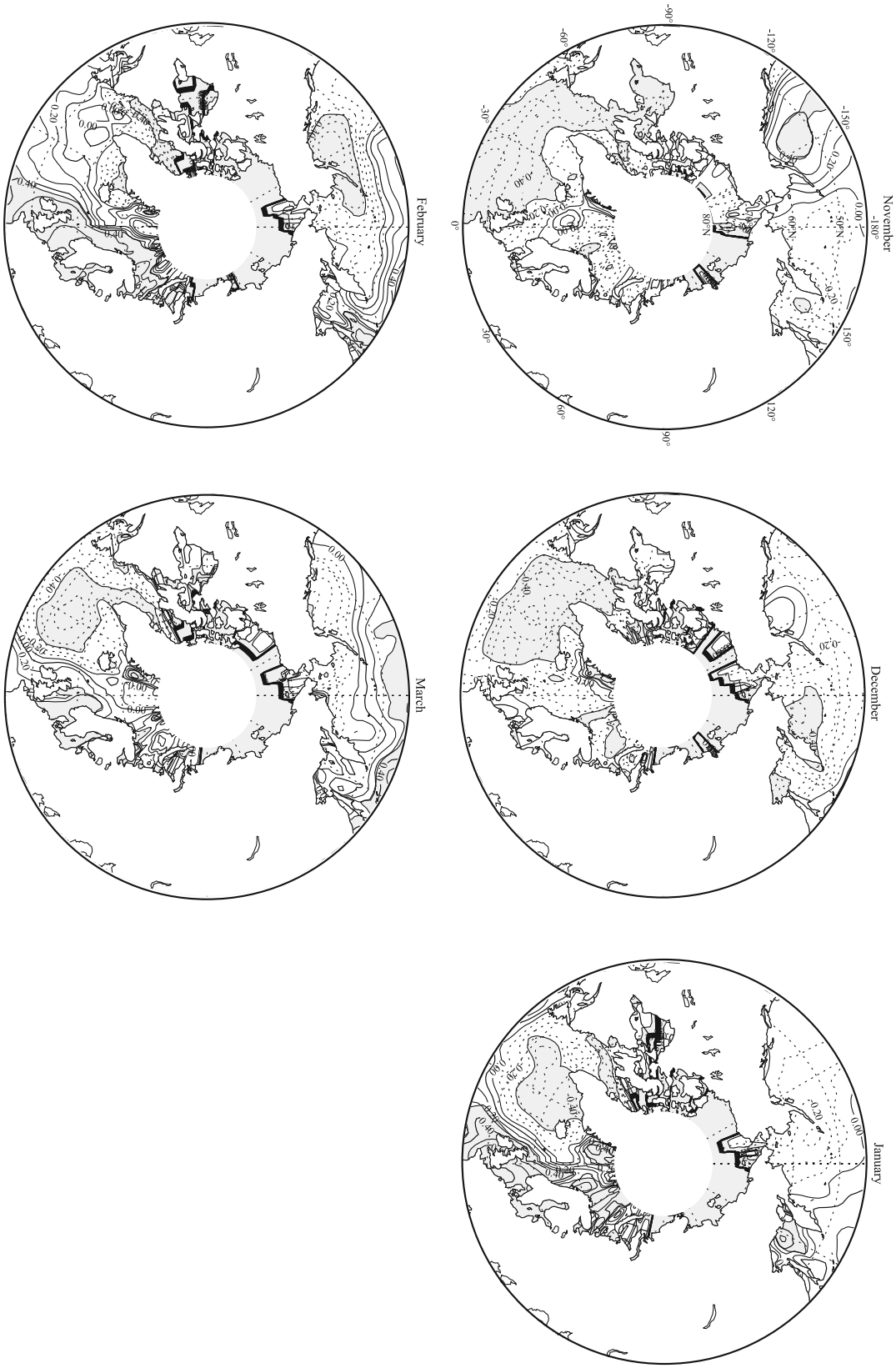

Figure 5. Distribution of correlation coefficients of SST between November and March versus the NAO index. Correlation coefficients have been computed for the 1979–2001 period. Correlation coefficients above the 90% confidence level following a phase-scrambling procedure with 999 samples are shaded. See text for more details.

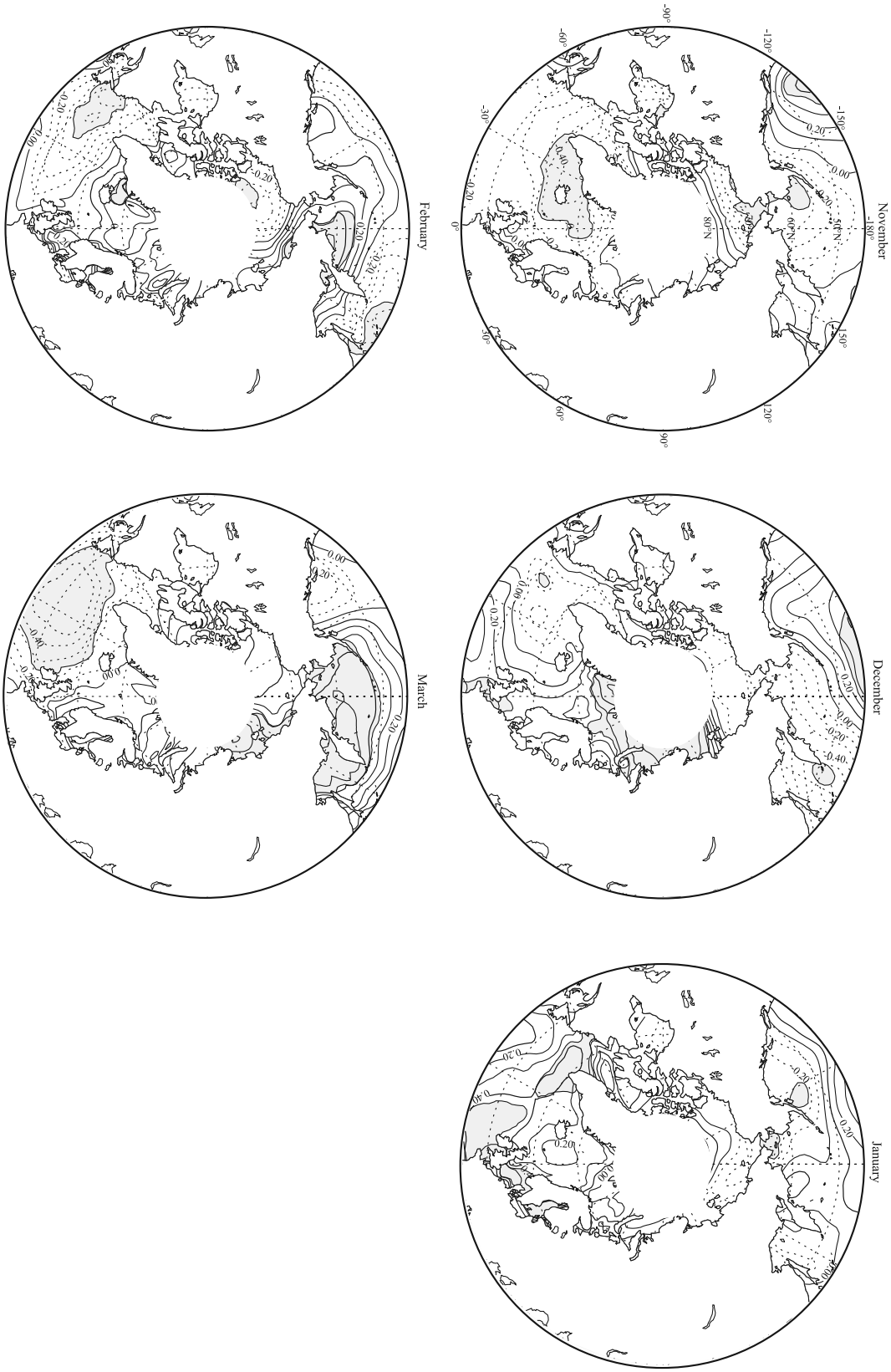

Figure 6. Distribution of correlation coefficients of the difference (SST-T500) between November and March versus the NAO index. Correlation coefficients have been computed for the 1979–2001 period. Correlation coefficients above the 90% confidence level following a phase-scrambling procedure with 999 samples are shaded. See text for more details.

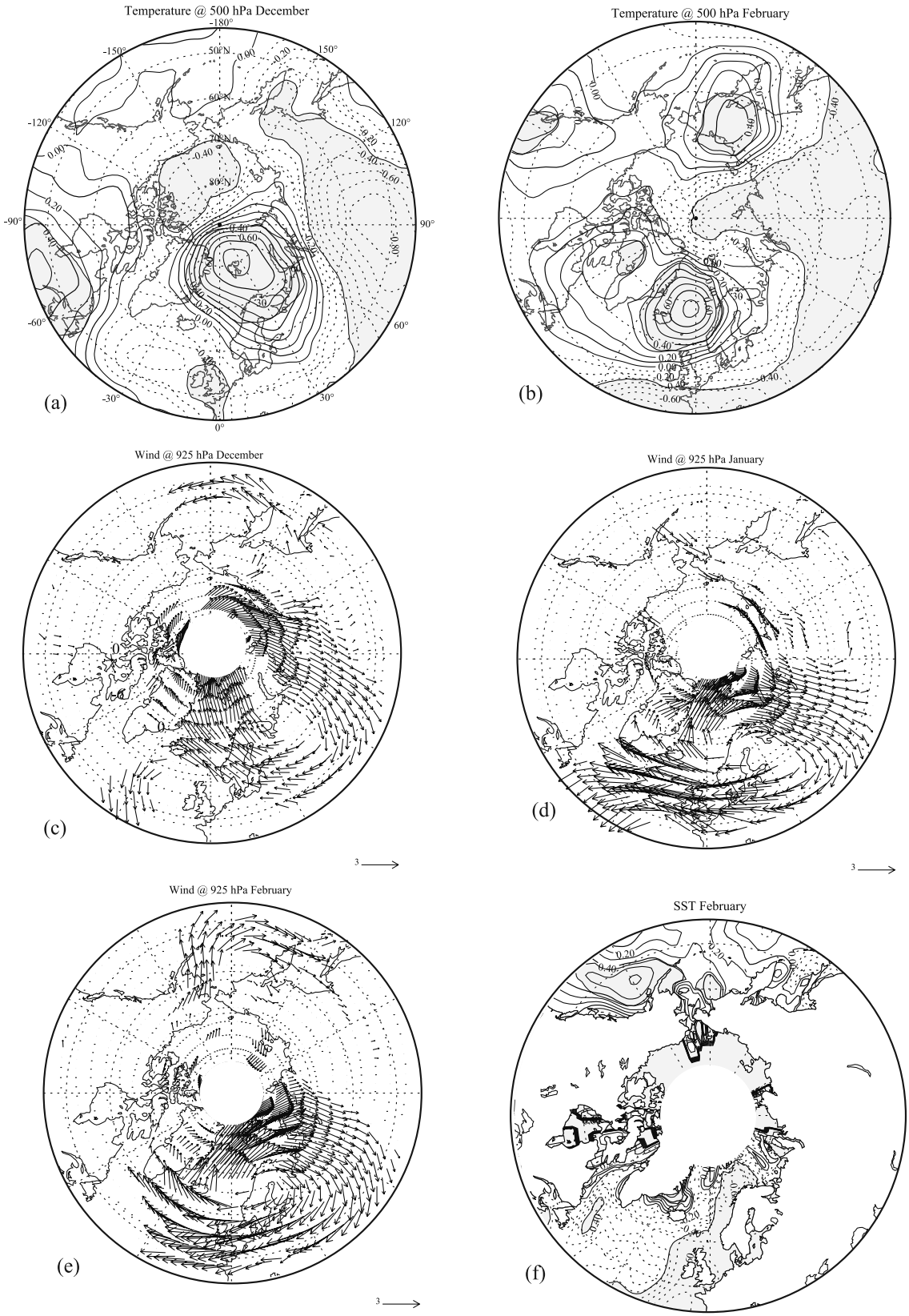

Figure 7. Distribution of correlation coefficients versus the SCAND index for (a) T 500 in December, (b) T 500 in February, (c) 925 hPa wind in December, (d) 925 hPa wind in January, (e) 925 hPa wind in February, and (f) SST in February.

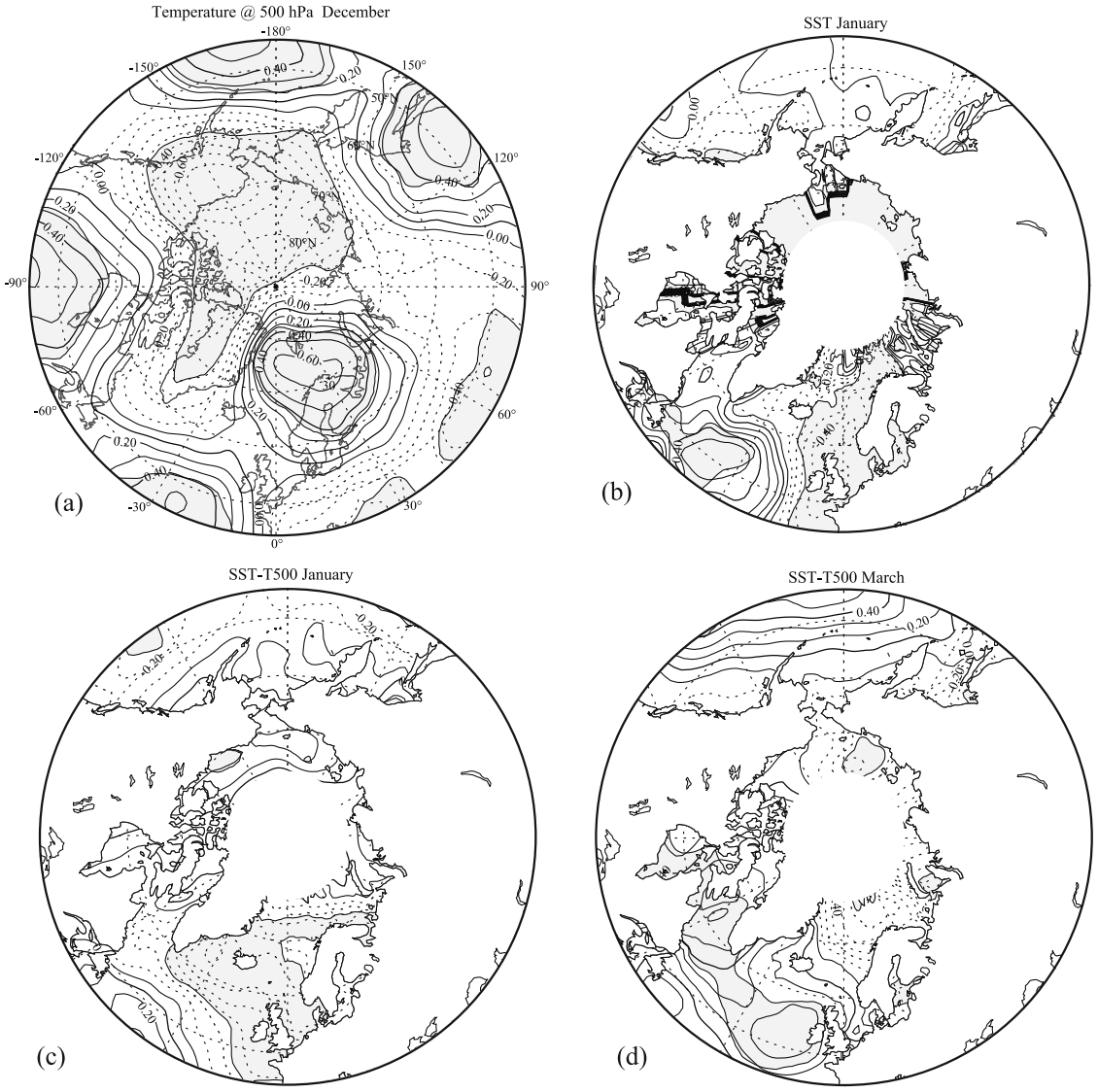

Figure 8. Same as Figure 7 but versus POLASIA and for (a) T500 in December, (b) SST in January, (c) (SST-T500) in January, and (d) (SST-T500) in March.

Atlantic. Accordingly, positive correlation patterns between the corresponding index and the temperature at 500 hPa are obtained to the west of the domain of interest and negative ones to the east. In November and January, significantly higher temperatures are found over most of the Norwegian Sea, while in November and February (Figure 9a), significantly lower temperatures are observed over the Barents Sea (correlation values of about −0.6).

[33] There is not much association between the East Atlantic/West Russia index and 925 hPa winds. The exceptions are for November (Figure 9b) and February over the Barents Sea, where a positive index corresponds to northeasterly winds, and January over the southern part of the Norwegian Sea corresponding to westerly winds.

[34] The East Atlantic/West Russia index also shows little association with the SST, with the exception of negative correlations over the Barents Sea at the end of the polar low season.

[35] It is correlated with (SST-T500) only in December and February (negative in December, positive in February, barely significant).

[36] Finally, the East Atlantic/West Russia index is associated with easterly 300 hPa winds over the North Atlantic at the beginning of the winter season, leading to a decreased likelihood of synoptic-scale storms, and therefore of polar lows over the Norwegian Sea.

3.2.4. East Atlantic Pattern

[37] In the positive phase of the East Atlantic pattern, synoptic activity is inhibited in the Nordic Sea, and enhanced to the south. This results in T500 becoming significantly correlated with the East Atlantic index generally at southern latitudes, compared to other indices. However, negative significant correlations are found in November (Figure 10a) over an area centered over Iceland, and in January (Figure 10b) over the Labrador Sea and the eastern Canadian waters (coefficients of about −0.7). In

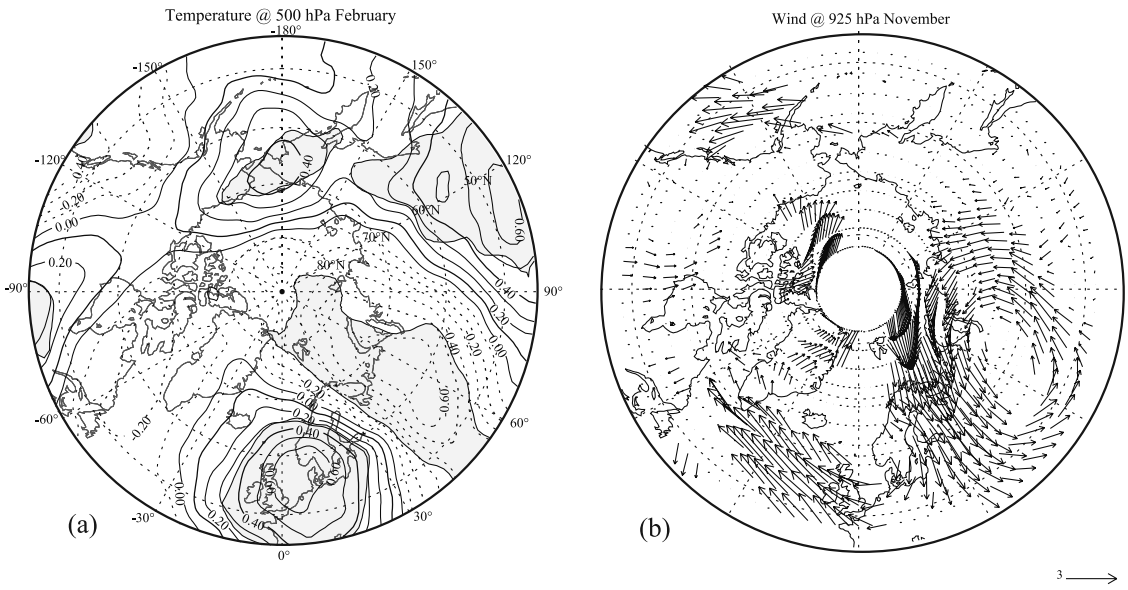

Figure 9. Same as Figure 7 but versus EAWR and for (a) T500 in February and (b) 925 hPa wind in November.

March, there is also a significant area over the Barents Sea, but correlation coefficients are lower (about −0.4).

[38] Concerning the 925 hPa wind, in November (Figure 10c) and January, a positive phase of the East Atlantic pattern is associated with northerly winds over the Davis Strait and Labrador Sea. Conversely, over the Norwegian Sea, it corresponds to either easterly or southerly winds in January, which do not favor polar low developments.

[39] There are significant positive correlations between the East Atlantic index and the SST in January over an area between Spitzbergen and northern Scandinavia, and in the following months over an area between Iceland and Norway (Figure 10d, valid for February). This will favor the formation of polar lows of predominantly convective nature.

[40] Correlations between the East Atlantic index and (SST-T500) are negative over eastern Canadian waters, but never significant except in January (Figure 10e); they are generally positive over the Norwegian Sea, and partly significant in December and January. Correlations over the Barents Sea are mostly negative, except in December, and not significant.

4. Summary and Concluding Remarks

[41] The North Atlantic region is prone to the development of polar lows which form when very cold air is transported over relatively warm open sea. Because the warming in the Arctic is expected to be larger than the global average [e.g., *Holland and Bitz*, 2003], it is important to assess its effect on severe weather over polar and subpolar areas. It is therefore necessary to understand the associations between large-scale environment and polar low activity. As a first step toward documenting these associations, standard cross-correlation and regression techniques between the corresponding indices and atmospheric fields have been performed. The statistical significance of the results has been carefully assessed taking into account the autocorrelation characteristics of the time series. The associations have been investigated separately for the months November until March, which correspond to the period of maximum polar low activity. The variables examined in this study are the temperature and geopotential height at 500 hPa, the wind at 925 hPa, the SST, the difference between the SST and air temperature at 500 hPa, and the wind at 300 hPa, which are known to have an influence on polar low developments, and are better represented in reanalyses than are the polar lows themselves [*Condron et al.*, 2006]. Upper level fields were provided by reanalyses (ERA-40 and NCEP-R2), and the SST from a monthly extended reconstruction of global SST based on Comprehensive Ocean-Atmosphere Data Set with improved high-latitude values.

[42] It is found that the NAO has a strong impact on all these variables, and therefore on the likelihood of polar low formation. In the Labrador Sea and the eastern Canadian waters, the positive phase of the NAO is associated with lower temperatures (and lower geopotential height) at 500 hPa, and a northerly flow, especially at the beginning of the season, both of which favor polar low formation. Over the Norwegian Sea, the influence of the NAO occurs more through the increase of synoptic activity, and the fact that several polar lows will form on the flank of synoptic storms, or through the creation of favorable conditions for reverse shear polar lows. Also over the Norwegian Sea, higher SST for positive NAO conditions from January onward will favor the formation of polar lows of predominantly convective nature, while to the east of Greenland, the reduction of sea ice plus the northerly low-level flow should lead to a larger number of polar lows to form. *Carleton* [1985, 1996] observed that fewer systems entered the British Isles and western Europe from the Atlantic when the NAO was in its positive phase; this is likely related to the lack of northerly flows added to the significant SST decrease to the southwest of the domain associated with this NAO phase. The Barents and Kara Seas polar low activity exhibits little association with NAO, except through the increase of SST and reduction of sea ice. All these results are consistent with the

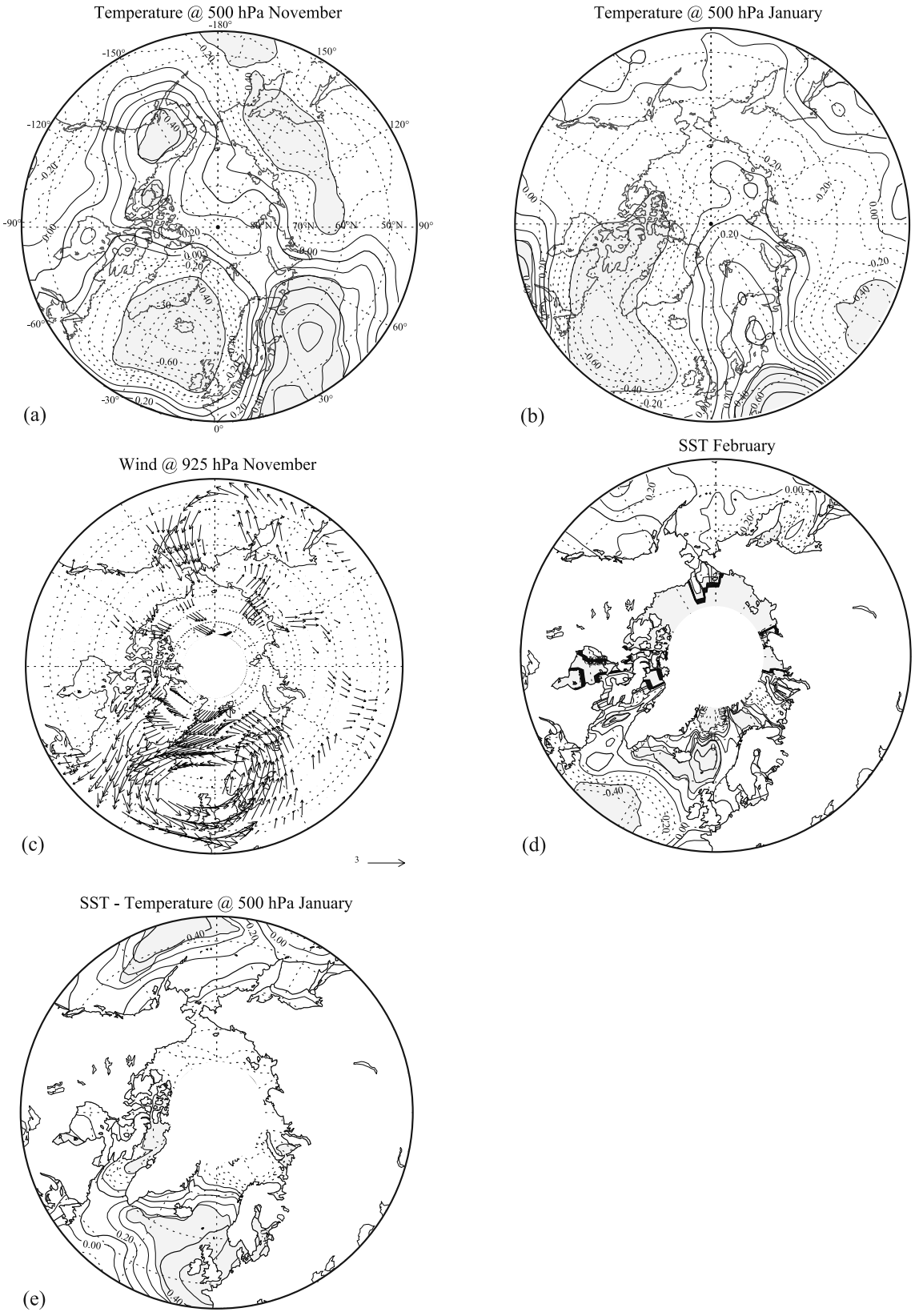

Figure 10. Same as Figure 7 but versus EASTATL and for (a) T500 in November, (b) T500 in January, (c) 925 hPa wind in November, (d) SST in February, and (e) (SST-T500) in January.

results obtained by *Carleton* [1985, 1996] and place them in a climatological context.

[43] In addition, our study shows that other teleconnection patterns also help determine polar low regimes. Of those, the Scandinavia pattern shows a strong negative association with the studied variables over the Norwegian and Barents Seas, but only marginally affects the Labrador Sea and the east Canadian waters. The presence of a blocking high over Scandinavia leads to warmer upper level temperatures over most of the area where polar lows form, generally colder SST and a decrease of (SST-T500), and low-level flow from the east or the southeast over a large part of the domain, except the Barents and Kara Seas. A positive phase of the Scandinavia pattern is also associated with a decreased likelihood of synoptic-scale storms, and therefore of polar lows over the Norwegian Sea. Polar lows which form over more southern regions may, however, be favored through the occurrence of lower 500 hPa temperatures and larger (SST-T500). The Polar/Eurasia pattern, which reflects the strength of the circumpolar vortex, has contrasting impact on polar low development. A strong vortex will tend to inhibit polar low genesis with colder SST from January onward and a global decrease of (SST-T500), with the exception of the 55–60°N latitude band at the end of the winter. The positive phase of the Polar/Eurasia pattern is associated with higher T500 over the Greenland/Norwegian and Barents Sea, that is especially significant in December and March. Its impact on cold air outbreaks is such that a strong vortex favors off-ice flow from the Arctic in November and February over the Barents Sea, and in March over the Kara Sea. In addition, in November, a positive phase of the Polar/Eurasia pattern is associated with equatorward flow over eastern Canadian waters while over the Norwegian Sea, the southwesterly flow can be conducive to reverse shear polar lows. The East Atlantic/West Russia pattern shows less association with polar low developments than the two previously discussed patterns. There is practically no significant association with SST and (SST-T500). The exception is for 500 hPa temperatures that are lower over the Barents/Kara Sea mainly in November and February, and to a certain extent in January (not significant in the latter case). The same months are characterized by northerly flow over these areas, which increases the likelihood of polar low formation. In January, reverse shear polar lows may be favored over the Norwegian Sea. Finally, a positive East Atlantic pattern promotes the genesis of polar lows at more southern latitudes, through colder 500 hPa temperatures, and the advection of very cold air over the Labrador Sea and Denmark Strait, but it has no big impact on higher latitudes. These results agree overall with those by *Harold et al.* [1999]; there are, however, some slight differences which are due to the fact that these authors consider mesocyclones for all seasons, while this study only considers those that are likely to be the most intense winter ones.

[44] The results presented above show the complexity of the associations between circulation teleconnections and variables associated with polar low formation, which vary both temporally and spatially. It is therefore important to study the links on a month-by-month basis, rather than averaging over several months, as it is usually the case. It must be also noted that in the areas where these relationships depend on sea ice extent and sea surface temperature, future changes due to climate change in either of these two variables are likely to alter these relationships, which adds to the complexity of the problem. It is hoped however that future very high resolution reanalyses or satellite imagery will permit to evaluate directly the association between the large-scale circulation and polar low occurrence and characteristics.

[45] **Acknowledgments.** Thanks are due to A. Carleton for reading an earlier version of the paper and to G. Noer for valuable discussions. The ERA-40 and NCEP-R2 reanalyses data sets were provided by ECMWF and the NOAA Climate Center (http://www.cdc.noaa.gov) through ClimServ. Thanks are due to S. Masson for providing graphical software (SAXO) for plotting the results.

References

Barnston, A. G., and R. E. Livezey (1987), Classification, seasonality and persistence of low-frequency atmospheric circulation patterns, *Mon. Weather Rev.*, *115*, 1083–1126.

Businger, S. (1985), The synoptic climatology of polar-low outbreaks, *Tellus, Ser. A*, *37*, 419–432.

Businger, S. (1987), The synoptic climatology of polar-low outbreaks over the Gulf of Alaska and the Bering Sea, *Tellus, Ser. A*, *39*, 307–325.

Carleton, A. M. (1985), Satellite climatological aspects of the polar low and instant occlusion, *Tellus, Ser. A*, *37*, 433–450.

Carleton, A. M. (1988), Meridional transport of eddy sensible heat in winters marked by extremes of the North Atlantic Oscillation, 1948/49–1979/80, *J. Clim.*, *1*, 212–223.

Carleton, A. M. (1996), Satellite climatological aspects of cold air mesocyclones in the Arctic and Antarctic, *Global Atmos. Ocean Syst.*, *5*, 1–42.

Carleton, A. M., L. A. McMurdie, K. B. Katsaros, H. Zhao, N. M. Mognard, and C. Claud (1995), Satellite-derived features and associated atmospheric environments of Southern Ocean mesocyclone events, *Global Atmos. Ocean Syst.*, *3*, 209–248.

Claud, C., N. M. Mognard, K. B. Katsaros, A. Chedin, and N. A. Scott (1993), Satellite observations of a polar low over the Norwegian Sea by Special Sensor Microwave/Imager, Geosat and TIROS-N Operational Vertical Sounder, *J. Geophys. Res.*, *98*, 14,487–14,506.

Claud, C., G. Heinemann, E. Raustein, and L. McMurdie (2004), Polar low *le Cygne*: Satellite observations and numerical simulations, *Q. J. R. Meteorol. Soc.*, *130*, 1075–1102.

Condron, A., G. R. Bigg, and I. Renfrew (2006), Polar mesoscale cyclones in the northeast Atlantic: Comparing climatologies from ERA-40 and satellite imagery, *Mon. Weather Rev.*, *134*, 1518–1533.

Davison, A. C., and D. V. Hinkley (1997), *Bootstrap Methods and Their Application*, 582 pp., Cambridge Univ. Press, New York.

Duncan, C. N. (1977), A numerical investigation of polar lows, *Q. J. R. Metorol. Soc.*, *103*, 255–267.

Emanuel, K. A., and R. Rotunno (1989), Polar lows as arctic hurricanes, *Tellus, Ser. A*, *41*, 1–17.

Ese, T., I. Kanestrom, and K. Pedersen (1988), Climatology of polar lows over the Norwegian and Barents Seas, *Tellus, Ser. A*, *40*, 248–255.

Forbes, G. S., and W. D. Lottes (1985), Classification of mesoscale vortices in polar airstreams and the influence of the large-scale environment on their evolution, *Tellus, Ser. A*, *37*, 132–155.

Hakkinen, S. (1995), Simulated interannual variability of the Greenland Sea deep water formation and its connection to surface forcing, *J. Geophys. Res.*, *100*, 4761–4770.

Harold, J. M., G. R. Bigg, and J. Turner (1999), Mesocyclone activity over the Northeast Atlantic. Part 2: An investigation of causal mechanisms, *Int. J. Climatol.*, *19*, 1283–1299.

Heinemann, G. (1996), A wintertime polar low over the eastern Weddel Sea (Antarctica): A case study with AVHRR, TOVS, SSM/I and conventional data, *Meteorol. Atmos. Phys.*, *58*, 83–102.

Hewson, T. D., G. C. Craig, and C. Claud (2000), Evolution and mesoscale structure of a polar low outbreak, *Q. J. R. Meteorol. Soc.*, *126*(A), 1031–1063.

Holland, M. M., and C. M. Bitz (2003), Polar amplification of climate change in coupled models, *Clim. Dyn.*, *21*, 221–232.

Kalnay, E., et al. (1996), The NCEP/NAR 40-year reanalysis project, *Bull. Am. Meteorol. Soc.*, *77*, 437–471.

Kanamitsu, M., W. Ebisuzaki, J. Woolen, S. K. Yand, J. J. Hnilo, M. Fiorino, and G. L. Potter (2002), NCEP-DOE AMIP-II Reanalysis (R-2), *Bull. Am. Meteorol. Soc.*, *83*, 1631–1643.

Kolstad, E. W. (2006), A new climatology of favourable conditions for reverse-shear polar lows, *Tellus, Ser. A*, *58*, 344–354.

Lieder, M., and G. Heinemann (1999), A summertime Antarctic mesocyclone over the Southern Pacific during FROST SOP 3: A meso-scale analysis using AVHRR, SSM/I, ERS and numerical model data, *Weather Forecasting*, *14*, 893–908.

McMurdie, L. A., C. Claud, and S. Atakturk (1997), Satellite-derived characteristics of Spiral and Comma-shaped southern hemisphere mesocyclones, *J. Geophys. Res.*, *102*, 13,889–13,905.

Noer, G., and M. Ovhed (2003), Forecasting of polar lows in the Norwegian and the Barents Sea, paper presented at 9th Meeting of the European Geophysical Society Polar Lows Working Group, Eur. Geophys. Soc., Cambridge, U. K.

Parker, N. (1991), *Polar Low Handbook for Canadian Meteorologists*, Environ. Canada, Edmonton, Can.

Parker, N. (1997), *Cold Air Vortices and Polar Low Handbook for Canadian Meteorologists*, Environ. Canada, Edmonton, Can.

Rasmussen, E. A., and J. Turner (2003), *Polar Lows: Mesoscale Weather Systems in the Polar Regions*, 612 pp., Cambridge Univ. Press, New York.

Rasmussen, E. A., C. Claud, and J. F. Purdom (1996), Labrador Sea polar lows, *Global Atmos. Ocean Syst.*, *4*, 275–333.

Rigor, I. G., J. M. Wallace, and R. L. Colony (2002), Response of sea ice to the Arctic Oscillation, *J. Clim.*, *15*, 2648–2663.

Rogers, J. C., and H. van Loon (1979), The seasaw in winter temperatures between Greenland and northern Europe. Part II: Some oceanic and atmospheric effects in middle and high latitudes, *Mon. Weather Rev.*, *107*, 509–519.

Simmons, A. J., and J. K. Gibson (2000), The ERA-40 project plan, *ERA-40 Proj. Rep. Ser. no. 1,* 63 pp., Eur. Cent. for Medium-Range Weather Forecasting, Reading, U. K.

Smith, T. S., and R. W. Reynolds (2003), Extended reconstruction of global sea surface temperatures based on COADS data (1854–1997), *J. Clim.*, *16*, 1495–1510.

Smith, T. S., and R. W. Reynolds (2004), Improved extended reconstruction of SST (1854–1997), *J. Clim.*, *17*, 2466–2477.

van Loon, H., and J. C. Rogers (1978), The seasaw in winter temperatures between Greenland and northern Europe, Part I: General description, *Mon. Weather Rev.*, *106*, 296–310.

Wu, B., J. Wang, and J. Walsh (2004), Possible feedback of winter sea ice in the Greenland and Barents Seas on the local atmosphere, *Mon. Weather Rev.*, *132*, 1868–1876.

Yarnal, B., and K. G. Henderson (1989a), A climatology of polar low cyclogenetic regions over the North Pacific Ocean, *J. Clim.*, *2*, 1476–1491.

Yarnal, B., and K. G. Henderson (1989b), A satellite-derived climatology of polar-low evolution in the North Pacific, *Int. J. Climatol.*, *9*, 551–566.

C. Claud and B. Duchiron, Laboratoire de la Meteorologie Dynamique/Institut Pierre-Simon Laplace, Ecole Polytechnique, F-91128 Palaiseau, France. (chclaud@lmd.polytechnique.fr)

P. Terray, Laboratoire d'Océanographie et du Climat: Expérimentations et Approches Numériques/Institut Pierre-Simon Laplace, F-75252 Paris, France.